Quantum Power Flow

Fei Feng, *Student Member, IEEE*, Yifan Zhou, *Member, IEEE*, and Peng Zhang, *Senior Member, IEEE*

***Abstract*—This letter is a proof of concept for quantum power flow (QPF) algorithms which underpin various unprecedentedly efficient power system analytics exploiting quantum computing. Our contributions are three-fold: 1) Establish a quantum-state-based fast decoupled model empowered by Hermitian and constant Jacobian matrices; 2) Devise an enhanced Harrow-Hassidim-Lloyd (HHL) algorithm to solve the fast decoupled QPF; 3) Further improve the HHL efficiency by parameterizing quantum phase estimation and reciprocal rotation only at the beginning stage. Promising test results validate the accuracy and efficacy of QPF and demonstrate QPF's enormous potential in the era of quantum computing.**

***Index Terms*—Quantum power flow, quantum computing, fast decoupled power flow.**

I. Introduction

TRADITIONAL tools for real-time operation of modern power systems, such as probabilistic power flow, $N-x$ security screening and Monte Carlo methods, remain to be intractable problems. Power flow equations, if solved by the classical direct iterative algorithms, scale with time as $O(N)$ for an $N \times N$ system [1]. However, tremendous amount of repetitive power flow calculations are needed to analyze the impact of uncertainties (e.g., output from distributed energy resources, fluctuating demands, and random failures or faults) through traditional methods such as probabilistic power flow, making the exiting approaches impossible to meet the real-time operation requirements [2].

Theoretically, quantum computing algorithms can achieve exponential speedups over classical methods using noisy-free quantum computers [3], [4]. This work is the first attempt of leveraging quantum supremacy to resolve the intractable challenge related to power flow calculations. The key innovation is to architect a practical quantum power flow (QPF) model and solver through an improved Harrow-Hassidim-Lloyd (HHL) [5] algorithm. This letter demonstrates QPF's potential to meet the growing needs of power flow calculation and support fast and resilient power system operations.

Manuscript received October 30, 2020; revised February 8, 2021; accepted April 27, 2021. Date of publication May 4, 2021; date of current version June 18, 2021. This work was supported in part by the Advanced Grid Modeling Program under the U.S. Department of Energy's Office of Electricity, in part by the US National Science Foundation under Grant OIA-2040599, and in part by Stony Brook University's Office of the Vice President for Research through a Quantum Information Science, and Technology Seed Grant. Paper no. PESL-00306-2020. *(Corresponding author: Peng Zhang.)*

The authors are with the Department of Electrical and Computer Engineering, Stony Brook University, Stony Brook, NY 11794-2350 USA (e-mail: fei.feng@stonybrook.edu; yifan.zhou.1@stonybrook.edu; p.zhang@stonybrook.edu).

Color versions of one or more figures in this article are available at https://doi.org/10.1109/TPWRS.2021.3077382.

Digital Object Identifier 10.1109/TPWRS.2021.3077382

II. Quantum Power Flow

A. Fast Decoupled QPF Formulation

Fast decoupled power flow [6] is a most widely used variant of Newton-Raphson power flow owing to its excellent computational efficiency and convergence performance. It adopts constant Jacobian matrices based on the fact that in a bulk power grid voltage angles are mainly related to active power and voltage magnitudes to reactive power, and thus reduces the costs for updating the Jacobian matrix in each iteration. Inspired by the fast decoupled approach, we extend the traditional power flow into a quantum computing model:

$$|\mathbf{V}^{-1}\Delta\mathbf{P}\rangle = \mathbf{B}'|\mathbf{V}\Delta\boldsymbol{\theta}\rangle \tag{1}$$

$$|\mathbf{V}^{-1}\Delta\mathbf{Q}\rangle = \mathbf{B}''|\Delta\mathbf{V}\rangle \tag{2}$$

where $|\cdot\rangle$ denotes the normalised quantum states, which will be futher explained in Subsection II-B; $\Delta\mathbf{V}$ and $\Delta\boldsymbol{\theta}$ are the differences of voltage magnitudes and angles, respectively; $\mathbf{B}'$ and $\mathbf{B}''$ are coefficient matrices derived from the admittance matrix. Given $\Delta\mathbf{V}$ and $\Delta\boldsymbol{\theta}$, power mismatches $\Delta\mathbf{S} = [\Delta\mathbf{P}, \Delta\mathbf{Q}]^T$ can be updated by

$$\Delta\mathbf{S} = \left[\mathbf{S} - \bar{\mathbf{Y}}(\boldsymbol{\theta}) \cdot \mathbf{V} \circ \mathbf{V}\right] \tag{3}$$

where $\mathbf{S} = [\mathbf{P}, \mathbf{Q}]^T$ represents the active/reactive power injections, $\bar{\mathbf{Y}}(\boldsymbol{\theta})$ is the admittance matrix, $\circ$ means Hadamard product.

B. HHL-Based QPF Algorithm

Apart from having constant Jacobian matrices, a striking feature of the QPF model is that $\mathbf{B}'$ and $\mathbf{B}''$ are both Hermitian and sparse. This allows for a direct translation of the classical power flow into the quantum language.

Taking (2) as an example, the spectral decomposition of $\mathbf{B}''$ can be devised as

$$\mathbf{B}'' = \sum_{i=1}^{\zeta} \lambda_i |b_i''\rangle\langle b_i''| \tag{4}$$

where λ_i and $|b_i''\rangle$ are the i^{th} eigenvalue and eigenvector of $\mathbf{B}''$. Written in the eigenbasis of $\mathbf{B}''$, $|\mathbf{V}^{-1}\Delta\mathbf{Q}\rangle = \sum_{i=1}^{\zeta} \alpha_i |b_i''\rangle$, which gives

$$|\Delta\mathbf{V}\rangle = \mathbf{B}''^{-1}|\mathbf{V}^{-1}\Delta\mathbf{Q}\rangle = \sum_{i=1}^{\zeta} \lambda_i^{-1}\alpha_i |b_i''\rangle \tag{5}$$

An improved HHL algorithm, as shown in Fig. 1, is developed to achieve the aforementioned QPF computations in three steps. Three registers (R_c, R_v, R_l) are initialized at the beginning of

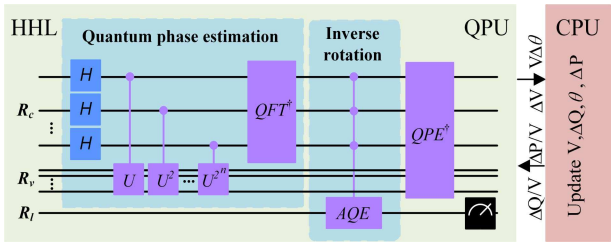

Fig. 1. Quantum circuit architecture for the HHL-based QPF algorithm.

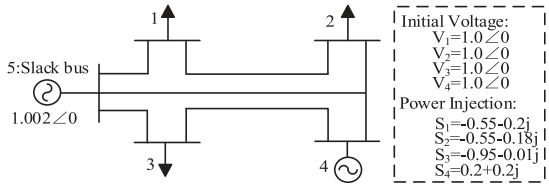

Fig. 2. Five-bus system for QPF tests.

QPF. R_c contains the binary representation of the eigenvalues of $\mathbf{B}'$ and $\mathbf{B}''$. R_v stores the qubit representation of $|\mathbf{V}^{-1}\Delta\mathbf{Q}\rangle$ and $|\mathbf{V}^{-1}\Delta\mathbf{P}\rangle$, and R_l regulates the angles of operators in ancilla quantum encoding (AQE) [3].

Step 1: Quantum phase estimation (QPE) It aims to determine the eigenvalue of unitary operators by using phase kickback and quantum inverse Fourier transform (QFT†). In the phase kickback, R_c is set to $|0\rangle$ and followed by Hadamard gates to provide superposition states [5]. If register R_c is $|0\rangle$, the controlled unitary operator does nothing to register R_v; if register R_c is $|1\rangle$, then the eigenvalues of controlled unitary operators can be kicked into $|1\rangle$ on register R_c. Eventually, quantum phase estimation can pick up the binary decimals of eigenvalue $|\lambda_i\rangle$. After QPE, a quantum state can be generated in the eigenbasis of $\mathbf{B}''$ as $\sum_{i=1}^{\zeta}\alpha_i|\lambda_i\rangle\otimes|b_i''\rangle$.

Step 2: Inverse rotation This step aims to kick the reciprocal of λ_i into state $|1\rangle$ for measurement. The reciprocal of eigenvalues from QPE can be achieved through the controlled operators in AQE : $|0\rangle\rightarrow\sqrt{1-\frac{C^2}{\lambda_i^2}}|0\rangle+\frac{C}{\lambda_i}|1\rangle$. Benefiting from invariant $\mathbf{B}'$ and $\mathbf{B}''$, the QPE and inverse rotation are parameterized only in the first iteration to update phase angle operators, significantly improving the efficiency of HHL.

Step 3: Inverse QPE (QPE†) The inverse QPE subroutine disentangles the register R_c to $|0\rangle$ by using controlled operator and leaves the remaining state as:

$$\sum_{i=1}^{\zeta}\alpha_i|0\rangle\otimes|b_i''\rangle\left(\sqrt{1-\frac{C^2}{\lambda_i^2}}|0\rangle+\frac{C}{\lambda_i}|1\rangle\right) \quad (6)$$

Once the measurement of R_l is $|1\rangle$, the corresponding iterative results $|\mathbf{V}\Delta\boldsymbol{\theta}\rangle$ and $|\Delta\mathbf{V}\rangle$ are in post-measurement states. Then, power flow variables $\boldsymbol{\theta}$, $\mathbf{V}$ can be updated for the next iteration. The QPF iterations continues until the mismatches $\Delta\mathbf{P}$ and $\Delta\mathbf{Q}$ achieve a convergence tolerance of ξ.

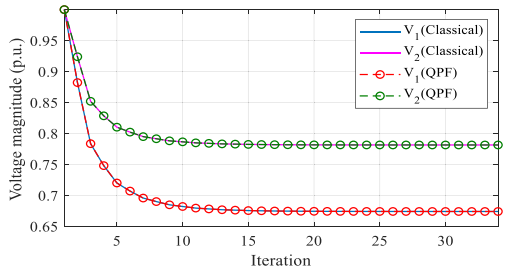

Fig. 3. Voltage profiles in Test II with different methods.

Algorithm 1: QPF Algorithm.

Initialize: $\boldsymbol{\theta}$, $\mathbf{V}$, $\mathbf{B}'$, $\mathbf{B}''$, $\mathbf{P}$, $\mathbf{Q}$, ξ;
while $\Delta\mathbf{P}$, $\Delta\mathbf{Q}\geq\xi$ **do**
  Update: $\Delta\mathbf{P}$, $\Delta\mathbf{Q}$ **Eq.** (3);
  if 1^{st} *iteration* **then**
    Input: $\mathbf{B}'$, $\mathbf{B}''$ $\Rightarrow$ HHL;
  end
  Input: $\Delta\mathbf{P}$, $\mathbf{V}$ $\Rightarrow$HHL $\Rightarrow$ $\Delta\boldsymbol{\theta}$;
  Input: $\Delta\mathbf{Q}$, $\mathbf{V}$ $\Rightarrow$HHL $\Rightarrow$ $\Delta\mathbf{V}$;
  Update: $\boldsymbol{\theta}$, $\mathbf{V}$;
end
Result: $\boldsymbol{\theta}$, $\mathbf{V}$ and the branch power flow.

QPF for the first time architect an AC power flow solution in quantum computers. **Algorithm 1** presents the pseudo code of QPF.

III. Case Study

The effectiveness and efficiency of QPF are verified on a five-bus test system (see Fig. 2). Test I/II verifies the QPF performance on normal and stressed conditions. QPF is implemented in IBM's Qiskit (0.23.4) where the number of R_c is set to 4.

A. Validity of QPF

This subsection verifies the correctness and convergence performance of QPF by comparing QPF results against those from classical fast decoupled power flow and Newton-Raphson's method. Table I presents the iteration process and the final power flow results under Test I. Fig. 3 shows the voltage convergence performance in Test II, where the load on bus 1 is increased to 2.2+0.8j p.u.. The following insights can be obtained:

- The QPF results are identical to the classical results, which validates the correctness and generality of QPF.
- The computation process shows that HHL exhibits satisfactory accuracy at each iteration. The reason is that sufficient quantum registers are employed for quantum eigenanalysis. In this case, if the number of quantum registers is lower than 4, QPF might fail to pick up accurate results.
- Compared with results under the normal condition, the iteration number in Test II is increased to 34. This is because the power system is close to solvability region boundary and its voltage profiles deteriorate.
- QPF inherits the convergence characteristics of the classical fast decoupled method, which is slightly weaker than

TABLE I
VOLTAGE PROFILES IN TEST I WITH DIFFERENT METHODS (P.U.)

Algorithm	Iteration	$\mathbf{V}_3$	$\mathbf{V}_4$	$\boldsymbol{\theta}_3$	$\boldsymbol{\theta}_4$
QPF	1	1.0141	1.0282	-0.1143	-0.0368
	2	0.9946	1.0181	-0.1139	-0.0340
	3	0.9950	1.0183	-0.1144	-0.0393
	4	0.9948	1.0182	-0.1144	-0.0393
	5	0.9948	1.0182	-0.1144	-0.0393
	6*	0.9948	1.0182	-0.1144	-0.0393
Classical Fast Decoupled	1	1.0141	1.0282	-0.1143	-0.0368
	2	0.9946	1.0181	-0.1139	-0.0340
	3	0.9950	1.0183	-0.1144	-0.0393
	4	0.9948	1.0182	-0.1144	-0.0393
	5	0.9948	1.0182	-0.1144	-0.0393
	6*	0.9948	1.0182	-0.1144	-0.0393
Classical Newton Raphson	1	1.0092	1.0251	-0.1136	-0.0382
	2	0.9951	1.0183	-0.1144	-0.0392
	3*	0.9948	1.0182	-0.1144	-0.0392

*Final power flow result.

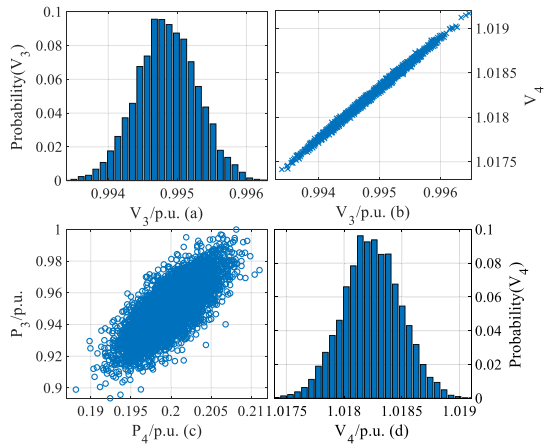

Fig. 4. Probabilistic voltages at buses 3 and 4 and their correlations (a) Probabilistic voltages at bus 3 (b) The correlation of voltages between buses 3 and 4 (c) The correlation of power injections between buses 3 and 4 (d) Probabilistic voltages at bus 4.

that of Newton's. This is because constant coefficient matrix can not adjust the calculation direction of QPF at each iteration. However, since the same convergence criteria is adopted for different power flow algorithms, the final power flow result of QPF is always as accurate as Newton's.

B. QPF-Based Stochastic Power Flow Analysis

This subsection extends QPF to the stochastic power flow analysis considering correlations between system variables. The power injections at buses 3 and 4 follow Gaussian probability distributions, where the correlation coefficient is set to be 0.75. The convergence tolerance is $\xi = 10^{-5}$.

Five thousand samples are generated randomly via Monte Carlo sampling. The probability distributions of voltage magnitudes at buses 3 and 4 as well as their correlations are obtained from QPF, as shown in Fig. 3.

- QPF is promising to be employed for stochastic power flow analyses. For instance, it can be seen that the voltage magnitude of bus 3 follows Gaussian distribution. Various correlation and dependence (i.e. Copulas, Pearson analysis) models can be readily integrated into QPF to obtain precisely the probability distributions of system states. Therefore, in the future QPF can serve as a potent tool for probabilistic system analyses. It opens a door to quantum-enabled, unprecedentedly efficient risk assessment and reliability analysis for electric grids.
- QPF will show unprecedented computational efficiency in repetitive power flow calculations. The time complexity of classical power flow algorithm at each iteration (i.e., solving linear equations on classical computers) is $O(N)$, while QPF acquires an exponential speedup resulting in $O(log(N))$. This supremacy will be more striking for ultra-scale power systems and high-dimensional uncertainties.

QPF is still under theoretical development as it still encounters excessively large depth of quantum circuit and short coherence time in today's noisy-intermediate-scale quantum (NISQ) computers. Nevertheless, QPF lays the foundation for power flow analysis on noisy-free quantum computers of a distant future.

IV. CONCLUSION

This letter opens the door for power system quantum analytics by developing a QPF algorithm. A fast decoupled QPF model is devised and solved by an enhanced HHL algorithm. QPF is a general approach for arbitrary AC power systems, and the proof-of-concept on a small test system has been successful. Despite existing gaps for practical applications of QPF in system operations and planning due to large quantum depths, short coherence times and noises on today's quantum computers, QPF lays solid foundation for power system analytics on the next generation quantum computers with much lower noises and computational power. It is expected to grow into a enormously useful tool for energy management and security analysis.

ACKNOWLEDGMENT

The authors would like to thank the Brookhaven National Laboratory operated IBM-Q Hub.

REFERENCES

[1] H. W. Dommel, *Notes on power system analysis*, The University of British Columbia, 1975.
[2] P. Zhang, W. Krawec, J. Liu, and P. Krstic, "ASCENT: Quantum grid: empowering a resilient and secure power grid through quantum engineering," Proposal# 2023915, Nat. Sci. Found., Feb. 2020.
[3] M. A. Nielsen and I. L. Chuang, *Quantum Computation and Quantum Information*. Cambridge, U.K.: Cambridge Univ. Press, 2011.
[4] C.-C. Chen, S.-Y. Shiau, M.-F. Wu, and Y.-R. Wu, "Hybrid classical-quantum linear solver using noisy intermediate-scale quantum machines," *Sci. Rep.*, vol. 9, Nov. 2019, Art. no. 16251, doi: 10.1038/s41598-019-52275-6.
[5] A. W. Harrow, A. Hassidim, and S. Lloyd, "Quantum algorithm for linear systems of equations," *Phys. Rev. Lett.*, vol. 103, no. 15, 2009, Art. no. 150502.
[6] B. Stott and O. Alsac, "Fast decoupled load flow," *IEEE Trans. Power App. Syst.*, vol. PAS-93, no. 3, pp. 859–869, May 1974.